scientific reports

Check for updates

OPEN

mRNA encoding bone morphogenetic protein-2 facilitated peri-implant bone formation of titanium implants placed in rat femurs

Kanoksiri Jriyasetapong[1], Nopparada Lawtrakulngam[1], Philaiporn Vivatbutsiri[2], Sunporn Namano[3], Kamolporn Wattanasirmkit[1], Somphote Angkhanawiriyarak[3] & Jaijam Suwanwela[1,3]✉

This study evaluated the effectiveness of N1-methylpseudouridine-modified mRNA encoding bone morphogenetic protein-2 (BMP-2 mRNA-LNP) in promoting bone growth and improving titanium implant integration in rat femur bone defects. Sixteen Sprague-Dawley rats (32 femurs) were used, with titanium wires implanted in the femoral defects. The defects were divided into four groups ($n = 8$): 5 µg BMP-2 mRNA-LNP, 15 µg BMP-2 mRNA-LNP, recombinant BMP-2 (rhBMP-2), and Dulbecco's phosphate-buffered saline (dPBS). Following euthanasia at 3 and 6 weeks, Micro-Computed Tomography (micro-CT) was performed to assess bone volume, trabecular architecture, and bone-to-implant contact. Push-out mechanical testing determined the maximal loading force for implant dislodgment, while elemental analysis using Energy-Dispersive X-ray Spectroscopy (EDS) and Scanning Electron Microscopy (SEM) assessed mineralization on the titanium surfaces. The 15 µg BMP-2 mRNA-LNP group demonstrated significantly enhanced bone volume, trabecular thickness, and bone-to-implant contact compared to the control group ($p < 0.05$). Additionally, this group showed higher calcium and phosphorus content, indicating superior mineralization. Concomitantly, the mean maximal loading force (N) increased in the BMP-2 mRNA-LNP group, though this increase was not statistically significant. These results suggest that BMP-2 mRNA-LNP offers a promising approach to enhance peri-implant bone formation and bone regeneration. While the 15 µg group showed slightly greater bone formation, most experimental parameters showed no significant differences compared to the 5 µg group, suggesting the lower dose may offer a more cost-effective approach without compromising efficacy.

Keywords Bone morphogenetic Protein-2 (BMP-2), Dental implant, Bone regeneration, Peri-implant bone formation, mRNA, Preclinical studies

Periodontal disease and the development of deep dental pockets are significant contributors to tooth loss, a condition that substantially impacts a patient's quality of life, alongside other factors such as dental caries[1]. Presently, dental implants have become a widely accepted option for missing teeth substitution[2]. The advantages include stimulating and maintaining the health of the jawbone while preserving the surrounding natural teeth. One of the major determinants of implant's long-term success is the degree of osseointegration that implant integrates with the surrounding bone[3].

Osseointegration, the bone healing process following dental implant insertion, involves four phases: hemostasis, inflammatory phase, proliferative phase, and remodeling. Throughout these stages, signaling molecules, including cytokines, extracellular matrix proteins, and small molecules, mediate coordinated interactions among various cell types that are crucial for successful osseointegration. Among these signaling molecules, Bone Morphogenetic Proteins (BMPs), a group within transforming growth factor-β family comprising

[1]Department of Prosthodontics, Faculty of Dentistry, Chulalongkorn University, Bangkok, Thailand. [2]Department of Anatomy, Faculty of Dentistry, Chulalongkorn University, Bangkok, Thailand. [3]Implant and Esthetic Dentistry Program, Faculty of Dentistry, Chulalongkorn University, Bangkok, Thailand. ✉email: Jaijam1220@gmail.com

of over 18 proteins, plays a critical role. BMP-2 has been widely used to induce osteogenic differentiation and endochondral ossification in mesenchymal stem cells (MSCs) to enhance bone regeneration[4–6]. A previous study on BMP-2 demonstrated higher cell mineralization in vitro and greater osseointegration in vivo compared with the control group in pig femurs after 2 weeks[7].

Recombinant human BMP-2 (rhBMP-2) acts as an osteoinductive agent to repair bone defects; however, the need for carrier agents, it's high cost, and the risk of enhancing the inflammatory reaction are its limitations[8–11]. Thus, messenger ribonucleic acid (mRNA) has emerged as an interesting alternative due to the drawbacks above[12,13]. The benefits of mRNA synthesis are that it is quick and cost-effective[14]. RhBMP-2 could deliver high-level protein production within a short translation time. Additionally, it restricts mutations and other undesirable genetic events associated with DNA by acting in a different compartment from the host genome, enhancing patient safety[15]. However, mRNA has some disadvantages, such as reduced stability, poor translation capacity and high immunogenicity[15]. These issues can be resolved by modifying nucleosides in the coding sequence. In this study, BMP-2 mRNA stability and translational capacity were enhanced by substituting uridine with N1-methylpseudouridine (m1Ψ), as reported by Andries et al. (2015)[16]. This modification effectively reduces cytotoxicity and immunogenicity while significantly improving protein translation and cellular viability. By addressing the inherent challenges of unmodified mRNA—such as instability, poor translational efficiency, and heightened immune responses—m1Ψ incorporation enables the development of safer and more effective mRNA-based therapies for bone regeneration[17,18]. Moreover, the mRNA in this study was delivered using chemical transfection with lipid nanoparticles (LNPs), which ionized lipids with greater properties. This method is recognized as the most widely utilized and efficient for mRNA delivery. It improves cell entry capacity and reduces degradation rates and toxicity that resulted in high levels of protein production over prolonged periods of translation[14–16,19–21]. Elangovan et al. (2015) showed that chemically modified mRNA (cmRNA) encoding BMP-2, delivered using non-viral vectors, is effective for bone regeneration in rats compared with plasmid DNA (pDNA) encoding BMP-2 via Micro-CT[12]. Additionally, another study demonstrated that intragingival injection of BMP-2 mRNA-LNP significantly increased the production of human BMP-2 proteins in rat gingival tissue compared with PBS[22].

Although BMP-2 mRNA has been evaluated for enhancing bone regeneration and healing[12], its effectiveness in promoting osseointegration for implants has not yet been investigated. In this study, we focus on peri-implant bone formation, which evaluates bone tissue growth in contact with the implant surface as an indicator of implant stability. The experiment was designed using titanium wires to represent dental implants with N1-methylpseudouridine-modified mRNA encoding BMP-2 (BMP-2 mRNA-LNP) placed in the rat femurs. The primary objective was to evaluate the effect of BMP-2 mRNA on the quality of peri-implant bone formation of rat femurs using micro-CT, push-out test, and EDS analysis. The main aim was to assess the effect of BMP-2 mRNA on the quality of peri-implant bone formation of rat femurs through the use of micro-CT, push-out testing, and EDS analysis.

Results

Micro-CT

The data were collected at 3 and 6 weeks after implantation. Micro-CT evaluation with image analysis software of the region of interest in 2D and 3D showed the bone volume and trabecular microarchitecture parameters, i.e., bone volume (BV), bone volume fraction (BV/TV), trabecular number (Tb.N), trabecular thickness (Tb.Th), and bone to implant contact (BIC). The bone formation in the 15 µg mRNA encoding BMP-2 group showed greater results in several parameters than the other three groups at both time points. (Fig. 1) Full-femur imaging prior to euthanasia was not performed. The analysis was limited to the peri-implant region of interest (ROI), as shown in the 3D reconstructions.

In 3-week rats, BV, BV/TV were significantly higher in the 15 µg mRNA encoding BMP-2 group compared with the other groups (p value < 0.05). Other parameters, i.e., Tb.Th, Tb.N and BIC were higher in the 15 µg mRNA encoding BMP-2 groups than the 5 µg mRNA encoding BMP-2, rhBMP-2 group and dPBS group, however, no significant differences were observed between the groups (p value < 0.05).

In 6-week rats, bone volume (BV), bone volume fraction (BV/TV), trabecular thickness (Tb.Th), and bone to implant contact (BIC) levels were significantly greater in the 15 µg mRNA encoding BMP-2 group compared with the control group (dPBS) (p value < 0.05). The trabecular number (Tb.N) was higher in the 15 µg mRNA encoding BMP-group than the 5 µg mRNA encoding BMP-2, rhBMP-2 and dPBS groups, however, the differences between the groups were not significant (p value < 0.05). (Fig. 2)

There were no significant differences observed in the same substances between 3 and 6 weeks (p value < 0.05). However, in general, in the rats treated with BMP-2, bone formation was greater at 6 weeks than 3 weeks in every parameter, except BV/TV (p value < 0.05). (Fig. 2)

Push-out test

The mean maximum loading force (N) was attained at the juncture where the applied force results in the initial dislodgement of the titanium wire from the rat's femur. The mean maximum loading force (N) for the 15 µg mRNA encoding BMP-2 group was higher than other groups at 3 and 6 weeks, however, the difference was not significant between the control and experimental groups (p value < 0.05). At 3 weeks, the 5 µg and 15 µg mRNA encoding BMP-2 groups exhibited higher maximum forces compared with the other two groups. However, at 6 weeks, only the 15 µg mRNA encoding BMP-2 group demonstrated a greater value than the other groups. The push-out value of implants in all groups demonstrated an increase at 6-weeks post-implant placement compared with the 3-week groups. None of these differences were significant (p-value < 0.05) (Fig. 3).

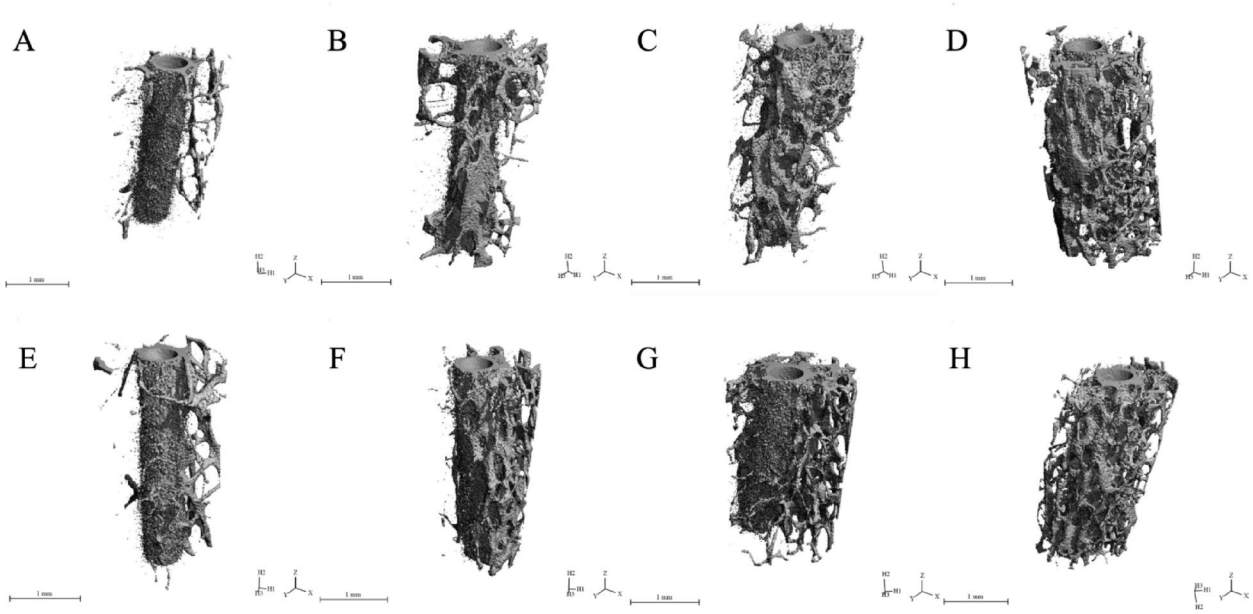

Fig. 1. Representative 3D reconstructed micro-CT images of bone volume around titanium implants at 3 weeks (A–D) and 6 weeks (E–H) after implantation. The region of interest (ROI) is centered around the implant. Images represent: dPBS group (A and E), rhBMP-2 group (B and F), 5 µg mRNA-BMP-2 group (C and G), and 15 µg mRNA-BMP-2 group (D and H). These images illustrate the peri-implant bone response for each treatment.

Energy-dispersive X-ray spectroscopy (EDS) & scanning electron microscopy (SEM)

After the push-out test, the dislodged titanium implant was analyzed using SEM/EDS. The surface elements of the implant predominantly consisted of titanium (Ti), calcium (Ca), phosphorus (P), and oxygen (O). The outcomes observed in the 3-week and 6-week groups demonstrated similar trends in the EDS results.

The weight% of titanium in the machined implants generally decreased from 3 to 6 weeks in almost every group, except for the dPBS group. The titanium percentage in the 15 µg mRNA encoding BMP-2 group was the lowest compared with the other groups and was significantly lower than the control group (dPBS) at 3 and 6 weeks (p value < 0.05), which is consistent with the micro-CT analysis. Furthermore, although the percentage of titanium in the 5 µg mRNA encoding BMP-2 group also decreased compared with the other two groups (rhBMP-2 and dPBS), the difference was not significant. (Fig. 4)

The calcium and phosphorus weight percentages in the retrieved machined implants from the 15 µg mRNA encoding BMP-2 group were significantly higher than those in the dPBS group at 3- and 6-weeks (p value < 0.05). The 5 µg mRNA encoding BMP-2 and rhBMP-2 also had higher weight percentages of calcium and phosphorus compared with the dPBS group. (Fig. 3)

Regression analysis indicated a positive correlation between the estimated tissue coverage area observed in EDS and BIC observed in micro-CT analysis ($R^2 = 0.684$) in the 6 week groups. These findings suggest the accuracy and precision of the EDS analysis method and micro-CT analysis for BIC within a 3–12 voxel distance. (Fig. 5)

High-magnification scanning electron microscopy (SEM) images revealed more well-developed tissue remnants on the implants in the experimental groups compared with the control groups. The interface tissue on the machined implants treated with dPBS, rhBMP-2, 5 µg mRNA encoding BMP-2 and 15 µg mRNA encoding BMP-2 is shown in Fig. 6.

Discussion

This study demonstrates BMP-2 mRNA's effectiveness in enhancing peri-implant bone formation, marking the first investigation of its application in this context. By evaluating bone regeneration and bone-to-implant contact at 3 and 6 weeks, we observed consistently higher micro-CT parameters—BV, BV/TV, Tb.N, Tb.Th, and BIC—in BMP-2 mRNA-treated groups compared to controls. These findings align with previous research highlighting BMP-2's pivotal role in bone regeneration and peri-implant bone formation in mammalian models. Prior studies with rhBMP-2 demonstrated accelerated bone healing and improved bone-implant contact, with significant increases in bone volume and density observed in histological and histomorphometric analyses[23,24]. Similarly, our study reinforces BMP-2's efficacy but offers a novel approach using mRNA to localize protein expression, potentially mitigating the systemic side effects associated with rhBMP-2.

In this study, peri-implant bone formation was assessed using micro-CT, push-out testing, and EDS/SEM, providing insights into bone volume, mineralization, and implant stability. However, these methods do not directly evaluate true osseointegration, which involves both mechanical interlocking and biological integration at the bone-implant interface[4–6]. To clarify this distinction, the term 'osseointegration' was replaced with "peri-

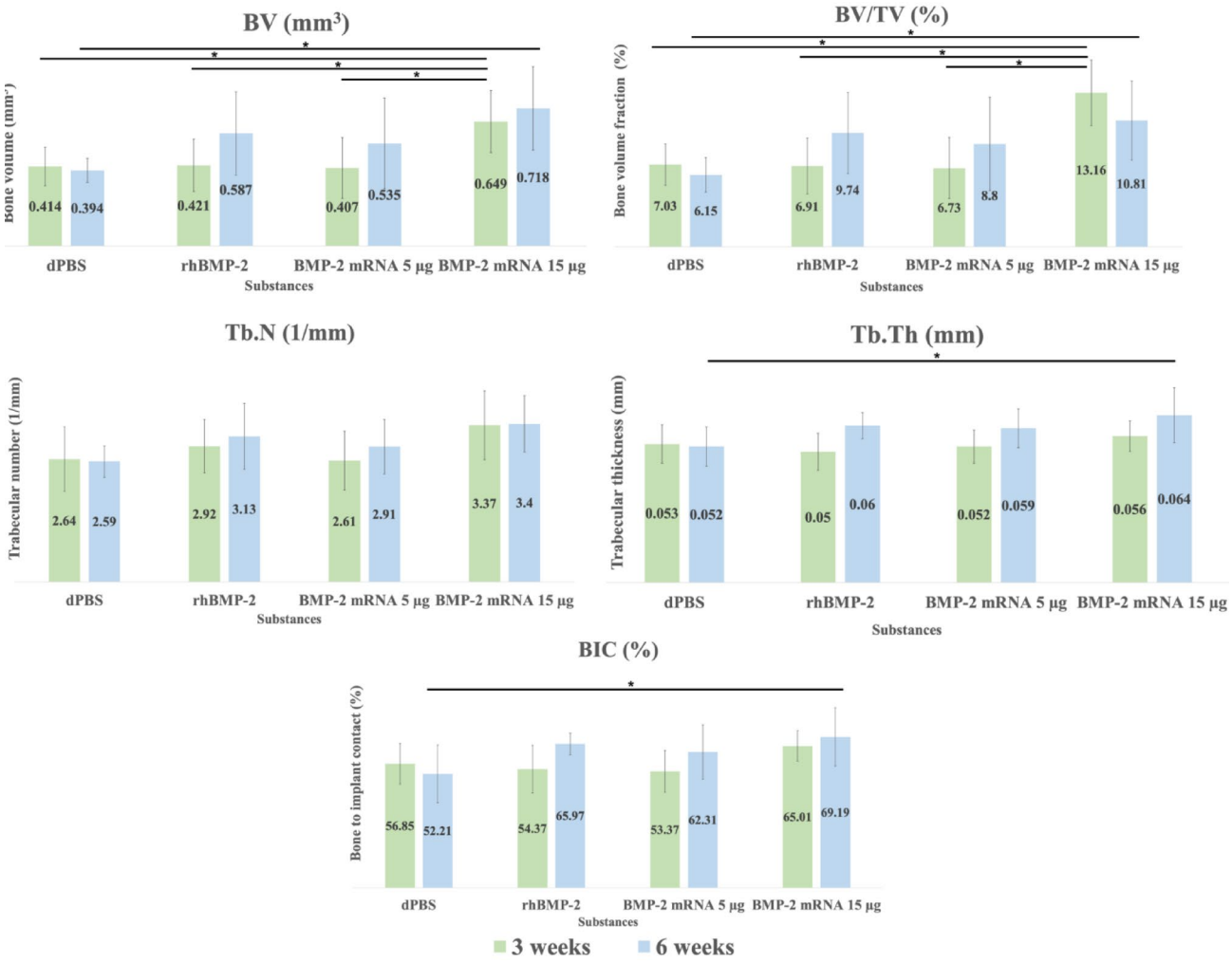

Fig. 2. Comparison of bone formation and trabecular micro-architecture at 3 and 6 weeks after implantation within the region of interest between groups. BV = bone volume; BV/TV = bone volume fraction; Tb.N = trabecular number; Tb.Th = trabecular thickness; and BIC = bone to implant contact. * indicates significant difference, $P < 0.05$.

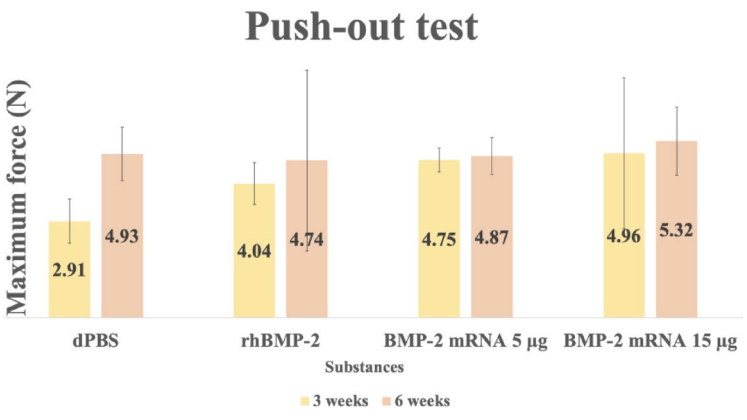

Fig. 3. Comparison of push-out test which performed maximum loading force (N) at 3 and 6 weeks after implantation within the region of interest between groups. *indicates significant difference, $P < 0.05$.

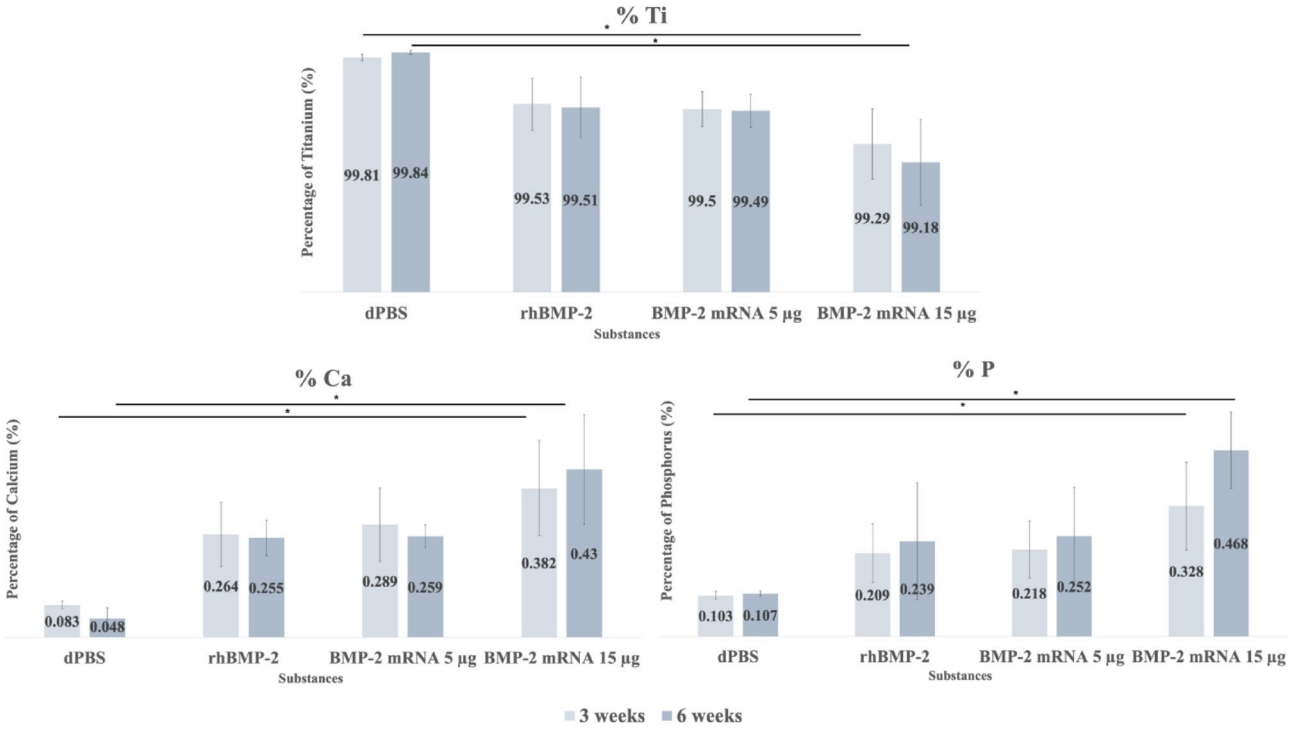

Fig. 4. Comparison of EDS elemental analysis percentage of a 3- and 6-week implant recovered after the push-out test between groups. The elements are Titanium, Calcium and Phosphorus, respectively. *indicates a significant difference, $P < 0.05$.

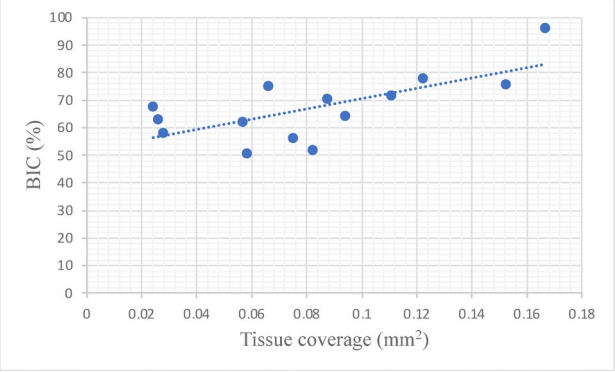

Fig. 5. Regression analysis indicated a positive correlation between the estimated tissue coverage area and Bone-to-Implant Contact (BIC) observed in micro-CT analysis ($R^2 = 0.684$) in 6 weeks group ($N = 14$), $P < 0.05$.

implant bone formation" throughout the manuscript. Future studies with porous titanium implants are planned for comprehensive assessment.

The 3- and 6-week time points were selected to evaluate early and mid-term bone healing, which are key for assessing initial intervention efficacy. BMP-2 promotes osteoblast differentiation and extracellular matrix production, especially during the first few weeks of healing[25]. In rats, significant bone healing activity typically occurs within 4 weeks, with peak cellular activity in the early reparative phase, during which mesenchymal stem cells differentiate into osteoblasts, and callus formation and mineralization occur. These processes support later stages of bone remodeling and long-term implant stability[26]. While our study focused on early healing, future studies extending to 12 weeks may reveal more about long-term regeneration and BMP-2 mRNA's full therapeutic potential.

Our findings show that BMP-2 mRNA concentration influenced outcomes, with the 15 µg group showing the best results and significant differences from the control in micro-CT and EDS analyses. However, most experimental parameters showed no significant differences between the 5 and 15 µg BMP-2 mRNA groups (p value < 0.05), except for BV and BV/TV, suggesting that the 5 µg dose may be more cost-effective without compromising efficacy. Further studies are needed to determine the optimal therapeutic dosage.

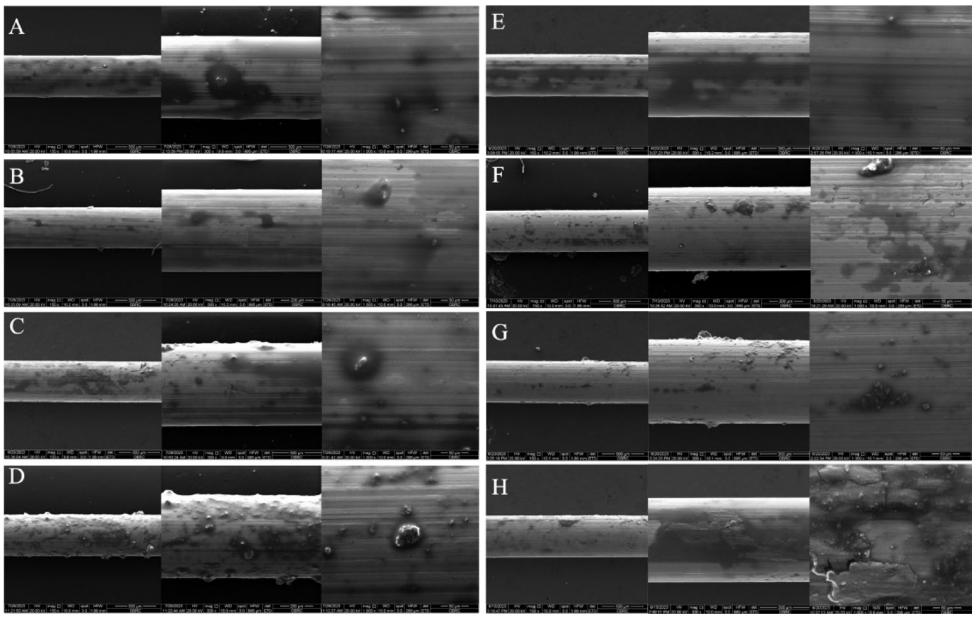

Fig. 6. Scanning Electron Microscopy (SEM) images of titanium implant surfaces at 3 weeks (A–D) and 6 weeks (E–H) post-implantation. Three levels of magnification (150x, 300x, 1000x) are shown for each group from left to right. Images represent: dPBS group (A and E), rhBMP-2 group (B and F), 5 µg mRNA-BMP-2 group (C and G), and 15 µg mRNA-BMP-2 group (D and H). These images show surface-level tissue coverage and morphology, contributing to interpretation of peri-implant integration.

BMP-2 mRNA demonstrates comparable efficacy to rhBMP-2 while offering additional advantages, including localized expression that minimizes systemic side effects like ectopic bone formation, inflammation, and swelling[11,12,20,27–29]. It is also more scalable and cost-effective due to in vitro transcription[14,15]. These benefits make BMP-2 mRNA a promising and economical alternative for clinical use.

Mechanistically, BMPs mediate osteogenesis via canonical and non-canonical pathways. In canonical signaling, BMPs bind to type I and II serine/threonine kinase receptors, forming a complex that phosphorylates Smad1/5/8. These R-Smads associate with Smad4, translocate to the nucleus, and regulate osteoblast differentiation through transcription factors such as PEBP2αA/Cbfa1. Non-canonical pathways, including the MAPK cascade, also influence gene expression[30,31]. BMP-2 primarily activates osteogenic genes through the Smad pathway, including Runx2, Osx, Col I, OPN, and OC[32,33].

This study represents the first instance of BMP-2 being directly injected into rat femurs without a carrier system. Previous studies on rhBMP-2 and BMP-2 mRNA have commonly used collagen or hydrogel scaffolds[34,35], which provide structural support for new bone formation and help maintain necessary shape and structure of the regenerating tissue[36]. However, these methods require a significant quantity of rhBMP-2, increasing costs and the risk of side effects such as inflammation and ectopic bone growth[37]. Additionally, the use of collagen can provoke immune responses, complicating its clinical application[38].

Considering these limitations and the long bone anatomy of the rat femur with its dense outer and spongy inner layers acting as a sealed compartment for BMP-2[39], scaffolds were not employed in this study. Instead, a direct injection technique was utilized, mimicking the clinical scenario of applying BMP-2 into a bone defect before implant placement. This method was efficient, straightforward, and aligned with the study's objectives while ensuring the rats' safety. Furthermore, encapsulating BMP-2 mRNA in LNPs through chemical transfection addressed challenges associated with scaffold use by enhancing mRNA stability, protecting against nuclease-mediated degradation, and promoting cellular uptake, ultimately improving treatment efficacy[19–21,40].

The significantly higher bone volume observed in the BMP-2 mRNA-LNP groups suggests potential benefits for enhancing local bone density at implant sites, particularly in osteoporosis patients with reduced skeletal mass due to imbalances in bone resorption and formation[41]. BMP-2 mRNA-LNP may help address this imbalance by promoting bone volume. Metallic artifacts limited bone-to-implant contact assessment[42,43], so we chose to measure BV/TV within 3–12 voxels, which correlated well with other parameters and tests.

Butz et al. (2006) reported strong correlation between BV/TV and histological bone structure within 3–30 voxels from the implant[44]. Additionally, Schouten et al. (2009) found artifacts near implants may overestimate bone volume. Thus, measuring from at least 3 voxels away helps ensure accuracy[45].

At 3 and 6 weeks post-implantation, experimental groups showed higher maximum forces than controls, though differences were not statistically significant ($p < 0.05$). Factors such as implant alignment, trimming precision, and small sample size may have influenced the results, despite use of an optimized rat femur model with standardized protocols including crosshead speed, trimming, and 2–3 mm bone exposure[46,47]. Moreover, push-out test accuracy can be affected by variables like jig fit, alignment, and bone mechanics[48,49]. The non-linear properties of bone further highlight the need for consistent testing conditions to minimize stress distribution

errors[50]. Although push-in tests better replicate chewing forces, the push-out method in this study enabled detailed elemental analysis of the titanium surface.

Peri-implant bone formation on smooth machined implants was evident by 3 weeks, as shown by micro-CT and EDS. SEM/EDS analysis of implants post push-out test revealed Ti weight percentages indicating exposed surface area. Bone-implant contact is typically greater near the metaphysis, where trabecular bone is abundant, than in the diaphysis of the rat femur[51]. To enhance accuracy, this research measured elemental percentages at three distinct points, calculating their average for greater accuracy.

The EDS analysis of exposed titanium weight percentages in the 6-week group positively correlated with average tissue coverage, aligning with BIC trends observed in micro-CT. This correlation highlights EDS as a potential surrogate measure for BIC[52,53]. High titanium levels indicated areas without peri-implant bone formation, while calcium and phosphorus presence suggested mineralized tissue and peri-implant bone formation.

The higher bone-to-implant contact in the 15 µg BMP-2 mRNA group at 6 weeks suggests greater bone formation compared to the 3-week group. However, limitations such as small sample size, optimal dosage, and study duration should be considered. This study did not address the implant's load-bearing function[53]. Future research should include longer durations and additional time points to better assess bone regeneration dynamics.

Future studies could improve precision by using one femur as control and the other as experimental, though this requires larger sample sizes. Additional analytic methods like histology, immunohistochemistry, and resonance testing could validate findings, as in prior rhBMP-2 studies[42,54,55]. Human studies are essential to translate BMP-2 mRNA findings from animal models to clinical practice and link micro-CT results to clinical outcomes. Future studies should also assess both short- and long-term effects of BMP-2 mRNA on bone healing and examine various implant types, such as SLA or rough surfaces, to improve clinical relevance.

Investigating different BMP-2 mRNA concentrations offers a promising direction for future research. Identifying the optimal dose to maximize efficacy while minimizing side effects is essential. Understanding the dose-dependent effects on peri-implant bone formation could enhance clinical outcomes, making BMP-2 mRNA a valuable tool in bone regeneration and clinical applications. Based on our findings, the 5 µg BMP-2 mRNA-LNP dose demonstrates comparable effectiveness to the higher dose and may serve as a more cost-effective and clinically practical option for peri-implant bone regeneration.

Materials and methods

Animal model

This study used sixteen male Sprague-Dawley (SD) rats, each 10 weeks old and weighing more than 250 g. The rats were procured from Nomura Siam International Co. Ltd (Bangkok, Thailand), and the experimental procedures were approved by the Animal Care and Use Committee of Chulalongkorn University Laboratory Animal Center (CULAC) (#2173019). All experimental procedures were performed in accordance with relevant institutional guidelines and regulations. This study is reported in accordance with the ARRIVE guidelines (https://arriveguidelines.org). The rats were accommodated in facilities with controlled lighting (Standard fluorescent) and temperature (21 ± 1 °C) receiving a standard rat diet and ad libitum access to water throughout both the preoperative and postoperative phases.

Implant design & production of mRNA encoding BMP-2 and rhBMP-2

Dental titanium implants were represented by grade 5 Eli ASTM F136 medical-grade titanium wires. These wires had an external diameter of 0.5 mm and a length of 10 mm (Fig. 7). The N1-methylpseudouridine modified mRNA encoding BMP-2 (m1ψ-BMP-2 mRNA) utilized in this study was provided by the University of Pennsylvania[56]. It is synthesized using a linearized plasmid DNA template, co-transcriptionally capped with CleanCap, and purified via cellulose-based chromatography. The uridine residues were substituted with N1-methylpseudouridine to enhance stability and reduce immunogenicity.

The mRNA was supplied in powder form, reconstituted in phosphate-buffered saline (PBS), and used at 5 µg and 15 µg in a total injection volume of 50 µL per femur[22]. The lipid nanoparticle (LNP) formulation used for encapsulation was based on a patented technology by Acuitas Therapeutics (WO2017004143), which enhances intracellular delivery via ionizable lipid components. These ionizable lipids become positively charged in the acidic endosomal environment, facilitating endosomal escape and cytoplasmic mRNA release.

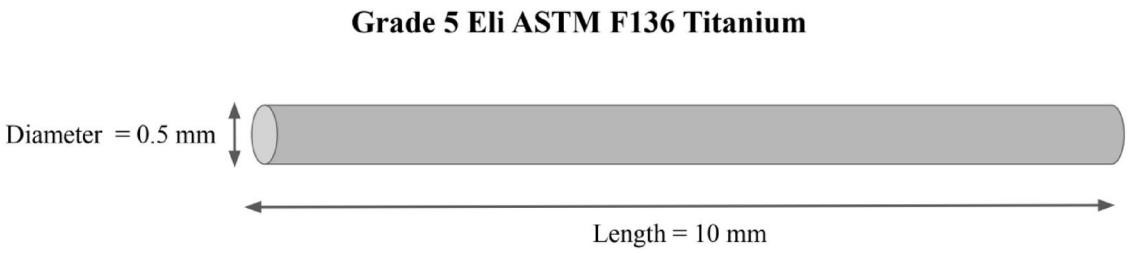

Fig. 7. Schematic presentation of the titanium implant wire used in this study (grade 5 Eli ASTM F136 titanium, 0.5 mm diameter, 10 mm length).

For rhBMP-2, this study used INFUSE® Bone Graft (rhBMP-2/ACS) from Medtronic Spinal and Biologics, Memphis, TN. Following the rhBMP-2 concentration of 0.08 µg/µL from a previous study by Angle et al. (2012)[57], a total of 4 µg rhBMP-2 was reconstituted in PBS and delivered in a 50 µL injection volume.

Surgical procedure

The rats underwent a one-week acclimatization period before the surgical procedures. 11-week-old male Sprague-Dawley rats were anesthetized with 2.0–5.0% isoflurane for surgery. Inhalation anesthesia was chosen due to the short surgical duration (25–30 min), allowing for rapid induction, easier control of anesthesia depth, and faster recovery. Compared to injectable agents, it also reduces the risk of overdose and prolonged sedation, making it more suitable for this animal model[58,59].

Preoperative analgesia comprised 12.5 mg/kg Tramadol. Anesthesia maintenance used 0.5-3% isoflurane. Local anesthesia involved a 2 mg/kg lidocaine injection along the incision line. A 10 mm incision at the knee joint exposed the distal femur after dislocating the patella.

The study utilized 16 Sprague-Dawley rats, resulting in 32 femurs that were randomly assigned to four different implant groups ($n = 8$ femurs per group): dPBS, 4 µg rhBMP-2, 5 µg BMP-2 mRNA-LNP[22], and 15 µg BMP-2 mRNA-LNP. The randomization of femurs and independent analysis of right and left knees ensured unbiased results. Titanium wires were implanted in the femoral defects, and the femurs were allocated as follows:

1. Micro-CT Analysis: All 8 femurs from each group were analyzed using micro-computed tomography (micro-CT) to assess bone volume (BV), bone volume fraction (BV/TV), trabecular number (Tb.N), trabecular thickness (Tb.Th), and bone-to-implant contact (BIC).
2. Push-out Mechanical Test: to evaluate the mechanical stability of the implants, 4 femurs from each group were subjected to the push-out test, where the maximum loading force required to dislodge the implant was recorded.

The titanium wires were prepared under sterile conditions. The defect holes were created using a 25 mm longitudinal hand drilling with a 25G gauge needle, aligned parallel the long axis of the bone to create a 0.6 mm circular hole from the distal side of the femur. Next, 50 µl of dPBS with different substances were injected into the respective group's femurs using a 27-gauge insulin needle. A titanium wire was implanted into the hole, and the opening site was closed using Bone wax W810 (Ethicon®, NJ, United States).

The knee joint was repositioned, and closure was performed in three layers: the joint capsule with interrupted 4/0 Monosyn sutures, the subcutaneous layer with subcuticular 4/0 Monosyn, and the outer skin layer externally with 4/0 nylon. Local anesthesia, 0.5% bupivacaine, was administered along the incision line. All procedures were conducted under antiseptic conditions. Two SD rats shared a cage with a partition. Subcutaneous injections of 5 mg/kg Carprofen or 12.5 mg/kg Tramadol were given for 2 days. For antibiotic prophylaxis, 10 mg/kg Enrofloxacin was injected daily for 5 days. Rats had access to food and water ad libitum, and the surgical wound was disinfected with Betadine daily. Sutures were removed after 7 days. At 3 and 6 weeks after implantation, the rats were euthanized through CO_2 inhalation. The rat femurs were collected, with the soft tissues removed, and the samples were disinfected using 2% chlorhexidine and 70% ethanol. A 13-millimeter section was cut from the femurs, 13 millimeters from the knee joint, using a carborundum disc. The sections were then promptly immersed in 10% neutral buffered formalin overnight and stored at 4 °C to preserve the biological tissue. (Fig. 8)

Micro-computed tomography imaging

Eight specimens from each group were immersed in 10% Phosphate-Buffered Saline (PBS), 10x concentration with a pH of 7.4. before micro-CT imaging in a high-resolution scanning mode was performed. The machine in this study was µCT 35 by Scanco Medical AG with setting of 70 kVp, 114 µA, 8 W, with a 6 µm voxel size. The scanning focused on a 4 mm area, located 6–10 mm from the insertion point of implant placement (Fig. 9A and B). The measurement area, centered around the implant, had a cylindrical shape (4 mm high, 2 mm diameter). Bone volume (BV) [mm^3], bone volume fraction (BV/TV) [%], trabecular number (Tb.N) [1/mm], trabecular thickness (Tb.Th) [mm], and BV/TV in a circumferential zone representing bone-to-implant contact (BIC) [%], were assessed[21].

Push-out test

The specimens were immersed in 70% formalin. Following saline rinsing, the rat femurs were placed in customized silicone putty indexes for support during trimming. To account for varying implant angulations, the femurs were viewed in relation to the horizontal plane by micro-CT scout view before cutting. The femurs were trimmed at the medial aspect to expose a 10-mm length from the insertion point to the end of the implant and the distal femur was further trimmed to expose a 3-mm length at the distal end of the implant by a dental carborundum diamond disc, a round steel bur, and #11 blade without overheating, maintaining a flat cross-sectional plane perpendicular to the implant path.

The customized blocks for this study were clear PVC tubes containing clear self-cure acrylic resin to secure the specimens. The block's lower half had a central tube for the titanium wire during the push-out test. After resin polymerization, the rat femur's medial aspect was vertically embedded in the block, exposing the distal part ~ 3 mm. A dental surveyor was used to evaluate the implant plane, and the upper part of the block was filled with clear self-cured resin, leaving ~ 1 mm of the distal femur exposed. The push-out test was conducted 24 hours post-polymerization.

The push-out test utilized a universal material testing system (EZ-S; SHIMADZU, Kyoto, Japan) with a custom stainless steel pushing rod (3 mm diameter) on a 500-N load cell. The push-out rod approached the specimen without touching it before applying the downward compression force. The load-displacement curve

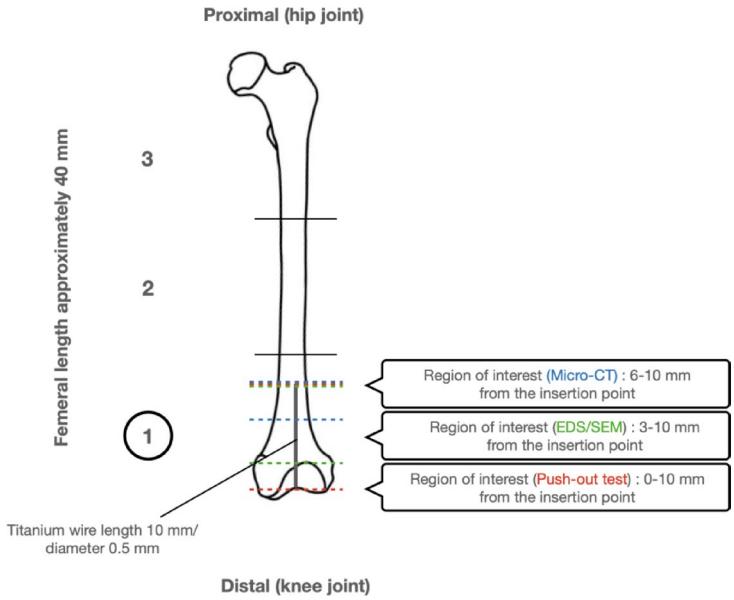

Fig. 8. The region of interest for micro-CT analysis extended from 6–10 mm in length from the insertion point. The region of interest for the push-out test extended from 0–10 mm in length from the insertion point. The region of interest for the EDS and SEM analysis extended from 3–10 mm in length from the insertion point.

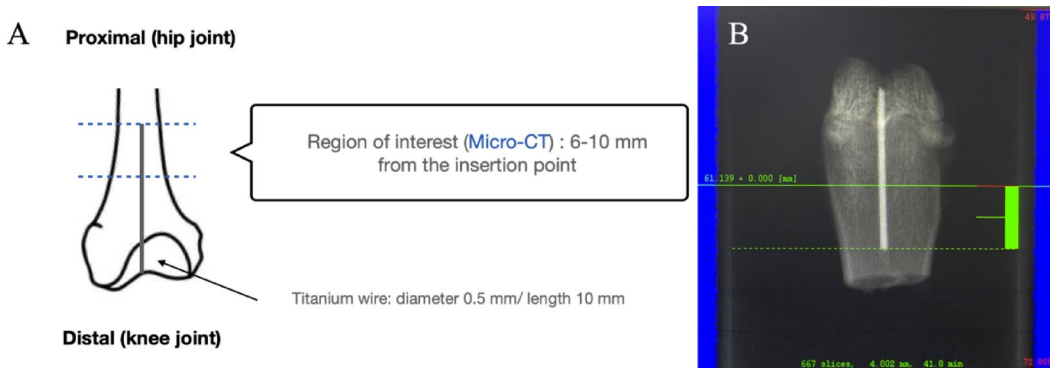

Fig. 9. The scanning focused on a 4 mm high area, located 6–10 mm from the insertion point of implant placement. **(A)** The schematic diagram of micro-CT analysis region. **(B)** Radiograph image showed the region of interest.

recorded the maximum loading force (N). The axial load on the implant was applied at a crosshead speed of 1 mm/min. The test was stopped before the pushing rod contacted the bone.

Energy dispersive X-ray spectroscopy (EDS) and scanning electron microscope (SEM)
Following the push-out test, the displaced titanium implants were retrieved from the femurs without washing[53]. The implant surfaces were scanned using Energy Dispersive X-ray Spectroscopy (EDS) with a Quanta 250 instrument from FEI, Oregon, USA. The settings of the machine in this present study were 20.00 kV and HV (High vacuum) mode. The EDS analysis comprised of three segments, covering the implant's entire length, excluding a 3-mm section exposed during the trimming for the push-out test to ensure precision in analyzing the elemental constituents. The mean measurements from these three segments were used to determine the elemental composition of titanium (Ti), calcium (Ca), and phosphorus (P) for each implant. The influence of the interface tissue coverage on the bone-to-implant contact of the implant was evaluated. The coverage area of the interface tissue was measured based on the Ti weight% across the entire implant surface: $2\pi r(100\text{-}Ti\%)/100$ (mm^2)[53]. The recovered implants underwent additional scrutiny via Scanning Electron Microscopy (SEM) using the Quanta 250 instrument from FEI, Oregon, USA. The settings of the machine in this present study were 20.00 kV and HV (High vacuum) mode[52,53,60].

Statistical analysis

This study utilized SPSS version 22.0 (SPSS Inc, Chicago, IL). One-way ANOVA, followed by Tukey's and Bonferroni post hoc tests, was employed to analyze data with a normal distribution and equal variance across the four groups. Statistical significance was determined at a 5% level (p-value < 0.05). Regression analysis was conducted to determine the relationship between the tissue coverage area and Bone-to-Implant Contact (BIC) as observed in the micro-CT assessment. Outcome assessments (micro-CT, push-out tests, SEM/EDS) were conducted by investigators blinded to experimental group assignments.

Data availability

The datasets generated and/or analyzed during the current study are available from the corresponding author on reasonable request.

Received: 21 September 2024; Accepted: 16 May 2025
Published online: 22 May 2025

References

1. Friel, T. & Waia, S. Removable partial dentures for older adults. *Prim. Dent. J.* **9** (3), 34–39 (2020).
2. Alghamdi, H. S. & Jansen, J. A. The development and future of dental implants. *Dent. Mater. J.* **39** (2), 167–172 (2020).
3. Nicholson, W. Titanium alloys for dental implants: A review. *Prosthesis* **2** (2), 100–116 (2020).
4. Albrektsson, T. & Albrektsson, B. Osseointegration of bone implants. A review of an alternative mode of fixation. *Acta Orthop. Scand.* **58** (5), 567–577 (1987).
5. Albrektsson, T., Hansson, H. A. & Ivarsson, B. Interface analysis of titanium and zirconium bone implants. *Biomaterials* **6** (2), 97–101 (1985).
6. Terheyden, H., Lang, N. P., Bierbaum, S. & Stadlinger, B. Osseointegration–communication of cells. *Clin. Oral Implants Res.* **23** (10), 1127–1135 (2012).
7. Teng, F. Y., Chen, W. C., Wang, Y. L., Hung, C. C. & Tseng, C. C. Effects of osseointegration by bone morphogenetic Protein-2 on titanium implants in vitro and in vivo. *Bioinorg. Chem. Appl.* **2016**, 3837679 (2016).
8. Balmayor, E. R. et al. Chemically modified RNA induces osteogenesis of stem cells and human tissue explants as well as accelerates bone healing in rats. *Biomaterials* **87**, 131–146 (2016).
9. Barr, T., McNamara, A. J., Sándor, G. K., Clokie, C. M. & Peel, S. A. Comparison of the osteoinductivity of bioimplants containing Recombinant human bone morphogenetic proteins 2 (Infuse) and 7 (OP-1). *Oral Surg. Oral Med. Oral Pathol. Oral Radiol. Endod.* **109** (4), 531–540 (2010).
10. Huntley, R., Jensen, E., Gopalakrishnan, R. & Mansky, K. C. Bone morphogenetic proteins: their role in regulating osteoclast differentiation. *Bone Rep.* **10**, 100207 (2019).
11. McKay, W. F., Peckham, S. M. & Badura, J. M. A comprehensive clinical review of Recombinant human bone morphogenetic protein-2 (INFUSE bone Graft). *Int. Orthop.* **31** (6), 729–734 (2007).
12. Elangovan, S. et al. Chemically modified RNA activated matrices enhance bone regeneration. *J. Control Release.* **218**, 22–28 (2015).
13. Gillman, C. E. & Jayasuriya, A. C. FDA-approved bone grafts and bone graft substitute devices in bone regeneration. *Mater. Sci. Eng. C Mater. Biol. Appl.* **130**, 112466 (2021).
14. Karikó, K., Ni, H., Capodici, J., Lamphier, M. & Weissman, D. mRNA is an endogenous ligand for Toll-like receptor 3. *J. Biol. Chem.* **279** (13), 12542–12550 (2004).
15. Patel, S. et al. Messenger RNA delivery for tissue engineering and regenerative medicine applications. *Tissue Eng. Part. A.* **25** (1–2), 91–112 (2019).
16. Andries, O. et al. N(1)-methylpseudouridine-incorporated mRNA outperforms pseudouridine-incorporated mRNA by providing enhanced protein expression and reduced immunogenicity in mammalian cell lines and mice. *J. Control Release.* **217**, 337–344 (2015).
17. Anderson, B. R. et al. Incorporation of Pseudouridine into mRNA enhances translation by diminishing PKR activation. *Nucleic Acids Res.* **38** (17), 5884–5892 (2010).
18. Karikó, K. et al. Incorporation of Pseudouridine into mRNA yields superior nonimmunogenic vector with increased translational capacity and biological stability. *Mol. Ther.* **16** (11), 1833–1840 (2008).
19. Kaczmarek, J. C., Kowalski, P. S. & Anderson, D. G. Advances in the delivery of RNA therapeutics: from concept to clinical reality. *Genome Med.* **9** (1), 60 (2017).
20. Pardi, N., Hogan, M. J., Porter, F. W. & Weissman, D. mRNA vaccines - a new era in vaccinology. *Nat. Rev. Drug Discov.* **17** (4), 261–279 (2018).
21. Stanton, M. G. Current status of messenger RNA delivery systems. *Nucleic Acid Ther.* **28** (3), 158–165 (2018).
22. Suppakitjareon, A. A., Mahanonda, R., Sa-Ard-Iam, N., Chanamuangkon, T. & Rek-yen P, W. W. In vivo protein expression after delivery of modified mRNA encoding bone morphogenetic protein – 2 into rat gingiva using different delivery systems: A pilot study. *J. Dent. Association Thail.* **72** (2), 7 (2022).
23. Bessho, K., Carnes, D. L., Cavin, R., Chen, H. Y. & Ong, J. L. BMP stimulation of bone response adjacent to titanium implants in vivo. *Clin. Oral Implants Res.* **10** (3), 212–218 (1999).
24. Jhin, M. J. et al. Ex vivo bone morphogenetic protein-2 gene delivery using bone marrow stem cells in rabbit maxillary sinus augmentation in conjunction with implant placement. *J. Periodontol.* **84** (7), 985–994 (2013).
25. Ingwersen, L. C. et al. BMP-2 Long-Term stimulation of human Pre-Osteoblasts induces osteogenic differentiation and promotes transdifferentiation and bone remodeling processes. *Int. J. Mol. Sci.* ;**23**(6). (2022).
26. Meyer, R. A., Meyer, M. H., Phieffer, L. S. & Banks, D. M. Delayed union of femoral fractures in older rats:decreased gene expression. *BMC Musculoskelet. Disord.* **2**, 2 (2001).
27. Sahin, U., Karikó, K. & Türeci, Ö. mRNA-based therapeutics — developing a new class of drugs. *Nat. Rev. Drug Discovery.* **13** (10), 759–780 (2014).
28. James, A. W. et al. A review of the clinical side effects of bone morphogenetic Protein-2. *Tissue Eng. Part. B Rev.* **22** (4), 284–297 (2016).
29. Zara, J. N. et al. High doses of bone morphogenetic protein 2 induce structurally abnormal bone and inflammation in vivo. *Tissue Eng. Part. A.* **17** (9–10), 1389–1399 (2011).
30. Ebara, S. & Nakayama, K. Mechanism for the action of bone morphogenetic proteins and regulation of their activity. *Spine (Phila Pa. 1976).* **27** (16 Suppl 1), S10–S15 (2002).
31. Wang, R. N. et al. Bone morphogenetic protein (BMP) signaling in development and human diseases. *Genes Dis.* **1** (1), 87–105 (2014).
32. Halloran, D., Durbano, H. W. & Nohe, A. Bone morphogenetic Protein-2 in development and bone homeostasis. *J. Dev. Biol.* ;**8**(3). (2020).

33. Sun, J., Li, J., Li, C. & Yu, Y. Role of bone morphogenetic protein-2 in osteogenic differentiation of mesenchymal stem cells. *Mol. Med. Rep.* **12** (3), 4230–4237 (2015).
34. Nguyen, P. D. et al. Scaffold-based rhBMP-2 therapy in a rat alveolar defect model: implications for human Gingivoperiosteoplasty. *Plast. Reconstr. Surg.* **124** (6), 1829–1839 (2009).
35. Yang, Z. et al. Hydrogel armed with Bmp2 mRNA-enriched exosomes enhances bone regeneration. *J. Nanobiotechnol.* **21** (1), 119 (2023).
36. Sheikh, Z., Javaid, M. A., Hamdan, N. & Hashmi, R. Bone regeneration using bone morphogenetic proteins and various biomaterial carriers. *Mater. (Basel).* **8** (4), 1778–1816 (2015).
37. Lin, H. et al. Efficient in vivo bone formation by BMP-2 engineered human mesenchymal stem cells encapsulated in a projection stereolithographically fabricated hydrogel scaffold. *Stem Cell. Res. Ther.* **10** (1), 254 (2019).
38. Hayashi, K., Yanagisawa, T., Kishida, R. & Ishikawa, K. Effects of scaffold shape on bone regeneration: tiny shape differences affect the entire system. *ACS Nano*. **16** (8), 11755–11768 (2022).
39. Nahian, A., Chauhan, P. R. & Histology *Periosteum and Endosteum. StatPearls. Treasure Island (FL): StatPearls Publishing. Copyright © 2024* (StatPearls Publishing LLC., 2024).
40. Zhang, W. et al. An improved, chemically modified RNA encoding BMP-2 enhances osteogenesis in vitro and in vivo. *Tissue Eng. Part. A*. **25** (1–2), 131–144 (2019).
41. Tang, C. H., Yang, R. S., Chien, M. Y., Chen, C. C. & Fu, W. M. Enhancement of bone morphogenetic protein-2 expression and bone formation by coumarin derivatives via p38 and ERK-dependent pathway in osteoblasts. *Eur. J. Pharmacol.* **579** (1–3), 40–49 (2008).
42. He, T. et al. A comparison of micro-CT and histomorphometry for evaluation of osseointegration of PEO-coated titanium implants in a rat model. *Sci. Rep.* **7** (1), 16270 (2017).
43. Liu, S., Broucek, J., Virdi, A. S. & Sumner, D. R. Limitations of using micro-computed tomography to predict bone-implant contact and mechanical fixation. *J. Microsc.* **245** (1), 34–42 (2012).
44. Butz, F., Ogawa, T., Chang, T. L. & Nishimura, I. Three-dimensional bone-implant integration profiling using micro-computed tomography. *Int. J. Oral Maxillofac. Implants*. **21** (5), 687–695 (2006).
45. Schouten, C., Meijer, G. J., van den Beucken, J. J., Spauwen, P. H. & Jansen, J. A. The quantitative assessment of peri-implant bone responses using histomorphometry and micro-computed tomography. *Biomaterials* **30** (27), 4539–4549 (2009).
46. Gao, Y. et al. Effect of combined local treatment with Zoledronic acid and basic fibroblast growth factor on implant fixation in ovariectomized rats. *Bone* **44** (2), 225–232 (2009).
47. Gao, Y. et al. Basic fibroblast growth factor suspended in matrigel improves titanium implant fixation in ovariectomized rats. *J. Control Release*. **139** (1), 15–21 (2009).
48. Black, J. Push-out tests. *J. Biomed. Mater. Res.* **23** (11), 1243–1245 (1989).
49. Castellani, C. et al. Bone-implant interface strength and osseointegration: biodegradable magnesium alloy versus standard titanium control. *Acta Biomater.* **7** (1), 432–440 (2011).
50. Dhert, W. J. et al. A finite element analysis of the push-out test: influence of test conditions. *J. Biomed. Mater. Res.* **26** (1), 119–130 (1992).
51. Soto-Peñaloza, D. et al. Effect on osseointegration of two implant macro-designs:A histomorphometric analysis of bicortically installed implants in different topographic sites of Rabbit's tibiae. *Med. Oral Patol. Oral Cir. Bucal.* **24** (4), e502–e10 (2019).
52. Kelly, J., Lin, A., Wang, C. J., Park, S. & Nishimura, I. Vitamin D and bone physiology: demonstration of vitamin D deficiency in an implant osseointegration rat model. *J. Prosthodont.* **18** (6), 473–478 (2009).
53. Morinaga, K. et al. Neuronal PAS domain 2 (Npas2) facilitated osseointegration of titanium implant with rough surface through a neuroskeletal mechanism. *Biomaterials* **192**, 62–74 (2019).
54. Senatov, F. et al. Osseointegration evaluation of UHMWPE and PEEK-based scaffolds with BMP-2 using model of critical-size cranial defect in mice and push-out test. *J. Mech. Behav. Biomed. Mater.* **119**, 104477 (2021).
55. Stadelmann, V. A., Conway, C. M. & Boyd, S. K. In vivo monitoring of bone-implant bond strength by MicroCT and finite element modelling. *Comput. Methods Biomech. Biomed. Engin.* **16** (9), 993–1001 (2013).
56. Vadovics, M., Muramatsu, H., Sárközy, A. & Pardi, N. Production and evaluation of Nucleoside-Modified mRNA vaccines for infectious diseases. *Methods Mol. Biol.* **2786**, 167–181 (2024).
57. Angle, S., Sena, K., Sumner, D., Virkus, W. & Virdi, A. Healing of rat femoral segmental defect with bone morphogenetic protein-2: A dose response study. *J. Musculoskel. Neuronal Interact.* **12**, 28–37 (2012).
58. Mook, D. *Anesthetic Management of Rodents and Rabbits* (Center for Laboratory Animal Resources, Morehouse School of Medicine, 2006).
59. Oh, S. S. & Narver, H. L. Mouse and rat anesthesia and analgesia. *Curr. Protocols*. **4** (2), e995 (2024).
60. Palmquist, A., Shah, F. A., Emanuelsson, L., Omar, O. & Suska, F. A technique for evaluating bone ingrowth into 3D printed, porous Ti6Al4V implants accurately using X-ray micro-computed tomography and histomorphometry. *Micron* **94**, 1–8 (2017).

Acknowledgements

This study was supported by the Faculty of Dentistry, Chulalongkorn University (Grant No. DRF65007) and Chulalongkorn University Laboratory Animal Center (CULAC). The authors declare no conflict of interest in connection with this study. The synthesis of N1-methylpseudouridine-modified mRNA encoding BMP-2 (m1ψ -BMP-2 mRNA) was kindly provided by Dr. Norbert Pardi from the University of Pennsylvania. We thank Dr. Kevin Tompkins for the critical review and language revision of this manuscript, and Dr. Naruedee Limpuangtip for statistical consultation. Figures 7, 8 and 9 were drawn by the authors. The authors also thank the Oral Biology Research Center and Dental Materials Research and Development Center, Faculty of Dentistry, Chulalongkorn University, for providing facility support.

Author contributions

K.J., N.L., P.V., and J.S. contributed to the conceptualization and design of the study. K.J., N.L., P.V., and J.S. were responsible for the methodology. K.J. and N.L. conducted the investigation. Formal analysis was performed by K.J. The original draft of the manuscript was written by K.J., and P.V., S.N., K.W., S.A., and J.S. contributed to the review and editing of the manuscript. Supervision was provided by J.S. All authors reviewed and approved the final manuscript.

Declarations

Competing interests

The authors declare no competing interests.

Additional information

Correspondence and requests for materials should be addressed to J.S.

Reprints and permissions information is available at www.nature.com/reprints.

Publisher's note Springer Nature remains neutral with regard to jurisdictional claims in published maps and institutional affiliations.